

Influence of alkali activator type and proportion on strength performance of calcined clay geopolymer mortar

Shinkafi, A. B., Khorami, M., Ganjian, E. & Tyrer, M.

Author post-print (accepted) deposited by Coventry University's Repository

Original citation & hyperlink:

Shinkafi, AB, Khorami, M, Ganjian, E & Tyrer, M 2021, 'Influence of alkali activator type and proportion on strength performance of calcined clay geopolymer mortar', *Construction and Building Materials*, vol. 267, 120446.

<https://dx.doi.org/10.1016/j.conbuildmat.2020.120446>

DOI 10.1016/j.conbuildmat.2020.120446

ISSN 0950-0618

Publisher: Elsevier

NOTICE: this is the author's version of a work that was accepted for publication in *Construction and Building Materials*. Changes resulting from the publishing process, such as peer review, editing, corrections, structural formatting, and other quality control mechanisms may not be reflected in this document. Changes may have been made to this work since it was submitted for publication. A definitive version was subsequently published in *Construction and Building Materials*, 267, (2021) DOI: 10.1016/j.conbuildmat.2020.120446

© 2020, Elsevier. Licensed under the Creative Commons Attribution-NonCommercial-NoDerivatives 4.0 International

<http://creativecommons.org/licenses/by-nc-nd/4.0/>

Copyright © and Moral Rights are retained by the author(s) and/ or other copyright owners. A copy can be downloaded for personal non-commercial research or study, without prior permission or charge. This item cannot be reproduced or quoted extensively from without first obtaining permission in writing from the copyright holder(s). The content must not be changed in any way or sold commercially in any format or medium without the formal permission of the copyright holders.

This document is the author's post-print version, incorporating any revisions agreed during the peer-review process. Some differences between the published version and this version may remain and you are advised to consult the published version if you wish to cite from it.

Influence of alkali activator type and proportion on strength performance of calcined clay geopolymer mortar

A. S. Bature^a, M. Khorami^a, E. Ganjian^a and M. Tyrer^a

^a Centre for Research in Built and Natural Environment, Coventry University, CV1 5FB, UK

ABSTRACT

The global abundance of low purity kaolin clay and the low embodied energy associated with its calcination makes it a promising aluminosilicate source that will extend the application of geopolymers. In this paper, the compressive strength and microstructure of iron rich, calcined clay based geopolymer mortars activated by two forms of sodium silicate (Na_2SiO_3) and sodium hydroxide (NaOH) solutions were studied and reported. The samples were cured either in the air or under sealed conditions. The result shows that the 28 days strength of the mortars achieved by reacting the calcined clay with hydrous sodium silicate powder, dissolved under normal atmospheric conditions and sodium silicate solution produced in a pressure reactor vessel are 0.5 MPa and 28.8 MPa respectively. The former produced a non-geopolymer mortar that has a discrete, undensified and uncompacted structure with heavy presence of residual particles, thus, achieving a strength that is 1.7% of the latter. The functional group analysis reveals that the binding phase of the peak strength mortar is ferro silicate (Fe-Si-O-Al).

Keywords: Calcined clay, sodium silicate, sodium hydroxide, geopolymer, mortar, compressive strength, microstructure.

1. Introduction

Alkali Activated Materials (AAM) have continued to receive attention as construction materials with lower CO_2 emissions that will further improve sustainability of the construction industry [1]. The most promising precursors for AAM are Ground Granulated Blast Furnace Slag (GGBS) and Fly Ash (FA) of adequate quality [2]. However, global supply of these materials is dwindling due to rapid decommissioning of coal thermal power plants in developed nations that generate Pulverized Fuel Ash (PFA) as a by-product and massive utilization of GGBS as Supplementary Cementitious Material (SCM) for Portland cement [3]. According to [1], calcined clay is presently the material with substantial potential to extend the availability of suitable minerals for AAM.

Over the past three decades, white metakaolin has been extensively studied as aluminosilicate source [4][5]. But, competing demand by different industries for high purity kaolin clay, high cost and intensive purification process are some of the factors limiting its availability to be used as either SCM or precursor for alkali activation [6]. Calcined clays are presently considered as cost-effective alternatives to high purity metakaolin clay and offer greater supply sustainability, due to the availability of vast clay reserves globally supplemented by clay waste generated by the ceramics industries and from construction projects [7]. Many of these clays have high iron contents and used to be considered unsuitable precursors for geopolymers [8], until recently, when research proved the viability of red geopolymer cement [9]. The iron content of kaolin clay is classified based on target application. In ceramic whiteware production, iron content of more than 0.9% is considered high and require intensive purification process. However, iron content of lateritic clay that can be used as precursor is considered high when it is more than 15% [10]. The clay used in this study has goethite and kaolinite content of 24.3% and 70.1% prior to calcination.

Alkali activation involves release of the aluminate (AlO_2^-) and silicate (SiO_4^{4-}) ions from an aluminosilicate source by reacting with alkali metal ions to produce hydrates of aluminosilicate (R-A-S-H, where R=Na or K) gel that form a solid mass when hardened and used as a binder [11]. Meanwhile, geopolymer, which is a sub-set of AAM, has distinct reaction governed by polycondensation rather than hydration. Geopolymer yield the bond: $\text{M}[-(\text{Si}-\text{O}_2)_z-\text{Al}-\text{O}]_n \cdot w\text{H}_2\text{O}$ where M is the alkaline element being Na, K, etc., n is the degree of polymerization and w is the amount of binding water [12]. While alkali activation produces a less stable structure with the presence of free end positive charge alkalis outside the structure, geopolymers produce a very stable 3-Dimensional (3D) polymeric network structure. For example, activating the calcined clay with sodium hydroxide solution alone will produce AAM, while activating with silicate-based activator such as Na_2SiO_3 solution formulated with the correct molar oxide composition will produce geopolymer. The binding phase of calcined clay is almost exclusively aluminosilicate that forms a highly coordinated 3D Si-O-Al polymeric network through polycondensation reactions typical of geopolymer binder [13]. According to [14], the binding phase for iron rich calcined clay geopolymers can be poly ferro sialate (Fe – Si – O – Al). [15]

reported that, the role of the Fe in this binding gel is beginning to be understood but require further study.

The binding phase and reaction product obtained from activation of calcined clay is determined by the type and dosage of alkali activator use in the reaction, mixing, curing method and duration, mineralogy of the clay, *etc.* For instance, [16] reported that increasing the SiO₂ to Na₂O molar ratio in a mix shifts the reaction towards the precipitation of more silicate species, forming complex polymeric structure that eases the development of a rigid framework. However, [17] concluded that the effect of increasing the SiO₂/Na₂O molar ratio above 2.5 on mechanical properties of geopolymers is limiting and degrading. Consequently, optimum alkali dosage (ratio of Na₂O to precursor) and modulus (ratio of SiO₂ to Na₂O) are essential in the alkalination of calcined clay, if geopolymers are to be achieved. [18] summarized the recommended optimal molar ratios compositional range for geopolymer product suitable for construction application to be: Si:Al of 3-5, Na:Al of 0.7-1.2 and H₂O:Na₂O of 12-18. However, even within the compositional range, the performance may vary significantly, which emphasize the need for the oxide optimization of any formulation.

Among the main factors limiting massive deployment of geopolymers in the construction industry is the utilization of highly alkaline liquid solutions that may pose some health and safety risks on site compared to the Portland binder [19]. Studies now focus on the development of powder activators, which can be dry mixed with a precursor to obtain “one-part” alkali activated binder that will require mixing with water only [2]. However, for silicate base alkali activators for instance, the anhydrous sodium silicate in powder form may require pressure reactor vessels to be adequately dissolved. On the other hand, the hydrous powder in principle may dissolve under normal atmospheric pressure conditions [20]. Accordingly, it is the extent of this dissolution that determines the availability of free silicate required for the geopolymerization process. Moreover, user friendly activators, that are produced from silicates with a molar ratio greater than 1.5 and are classified as irritant have shown great potential in extending the application of geopolymers [21][22].

Compressive strength is a basic property of mortar that corresponds very strongly with other mechanical and durability properties of paste, mortar and concrete [23]. Calcined clay based geopolymer mortars are often reported to achieve most of their strength within 7 days

depending on the alkali solution concentration, curing condition, *etc.* [24]. It is against this backdrop that this study compares the effects of the three forms of alkali activators and their proportion relative to the calcined clay content of the mixes, on the compressive strength and microstructure of the calcined clay geopolymer mortars cured in the air and under sealed conditions.

The alkali activators are: hydrous sodium silicate powder mixed with water under normal atmospheric pressure conditions that produced the desired solution for the alkalination; commercially available sodium silicate solution produced in a reactor; and sodium hydroxide solution prepared by adding water into the pellets that produced the solution of desired molarity. The precursor utilized in this study has the potential of satisfying the current and future demands of aluminosilicate sources in the UK. Recently, some studies have been reported that utilized rotary calcined lithomarge activated by potassium silicate solution to produce geopolymer mortar [25,26]. However, the difference in the calcination process and the type of activators used in this study provide a different perspective. Moreover, presently, there is serious research interest globally that seek to understand the role of iron (Fe) in the geopolymerisation phase of calcined lateritic clay. This challenge is partly due to the limitation of Nuclear Magnetic Resonance (NMR) spectroscopy in analysing the geopolymeric molecular structure because of the large iron content of the lateritic clay. Considering the impracticality of prescriptive recipe based standard for geopolymers due to its ability to utilize ever-growing range of materials [27], it is necessary to characterize the strength performance of this precursor considering different variables. The variables considered in this study are: formulation based on mass ratios derived from water demand of the precursor using three types of activators, and formulations based on the prescribed molar oxide ratios compositional range. Considering the growing interest for one-part geopolymers with hydrous metasilicates and sodium hydroxide as the common activators because of their potential to dissolve under atmospheric conditions, this study stresses the sensitivity of the calcined clay geopolymers synthesis to molar oxide composition.

2. Experimental methods

2.1. Materials

The calcined clay used for this study was supplied by Banah UK Ltd. The sourced clay was obtained from grinding the altered basalt – lithomarge in Northern Ireland [26]. It was processed from flash calcining low purity kaolin clay (70.1% kaolin content) at 750 °C and residence time of less than 1 s. The calcination resulted in the dehydroxylation and transformation of the goethite and magnetite phases of the precursor into hematite, but, maintained its layered structure. Even after activation with alkali metal source, metakaolin based geopolymer maintained its layered structure after the geopolymerization process (Dissolution, coagulation, polycondensation, gelation and crystallization). This is the reason why the reaction occurs at the surface of the geopolymers. This has already been reported by previous works [14,18]. The precursor particle sizes are 50% (d50) and 90% (d90) finer than 6 µm and 20 µm respectively. The calcined clay has 90% reactive elements, specific gravity of 2.89, specific surface (BET) of 75 m²/g and a loss on ignition of less than 2%. The pozzolanic activity of the calcined clay obtained from Chapelle Test is 972 mg CH /g, while the Strength Activity Index (SAI) based on ASTM C618 [28] was found to be 0.9. These measured values indicate that the precursor is highly pozzolanic [29]. Details of the precursor's pozzolanic characterization has been reported [30]. The oxide compositions of the calcined clay obtained from the XRF is presented in table 1. With iron content more than 15%, it's considered to be an iron rich precursor [10].

Table 1: Major oxide compositions (wt. %) of the calcined clay

Oxide (% by weight)	SiO ₂	Fe ₂ O ₃	Al ₂ O ₃	TiO ₂	MgO	CaO	Na ₂ O
Calcined clay	35.18	25.4	29.6	2.9	1.3	0.9	0.13

The sharp sand used as the fine aggregate component of the mortar was supplied by a local contractor and had particle sizes finer than 4.5 mm sieve size. NaOH reagent grade pellets of 97% purity and aqueous sodium silicate pentahydrate obtained from fisher scientific were used for the preparation of the alkali solution for the two groups of the mixes. The sodium silicate solution was prepared such that the quantity of the aqueous Na₂SiO₃ solid in the solution is 44.1%, while the 8M NaOH solution has 32% solid components and are both prepared 24 hrs prior to use. For the third group of mixes, commercially available sodium silicate solution

produced by Inoxia Ltd that has 54.5% solid component was used. This solution has the molecular ratio ($\text{SiO}_2/\text{Na}_2\text{O}$) of 2.05, which is classified as user-friendly [21].

2.2. Mixes

The mortar mixes were based on absolute volume method. The mortar density was the sum of the masses of all the materials in the mix per m^3 . Table 2 provides code and description of the mortar mixes, while the detailed proportions for the three groups are presented in table 3. The mass ratios of group 1 and 2 mixes were designed based on the water demand of the calcined clay. According to [31], the solution to precursors (S/P) mass ratio of metakaolin based geopolymers is generally close to 1, due to its water demand. This form the basis of using L:B ratios of between 0.7 and 1 in the two groups of mixes. On the other hand, the group 3 mixes were designed to satisfy the prescribed molar oxide ratios for geopolymers.

Table 2: Code and Description of the calcined clay geopolymer mortar mixes

Group	Sample code	Activator	Mix variable
1	CC – 32SH	NaOH solution made up of 32% solid	NaOH solution proportion in the mix varies from 0.8 to 1.0
	CC – 44.1SSP	$\text{Na}_2\text{SiO}_3 \cdot 5\text{H}_2\text{O}$ solution consisting of 44.1% solid	44.1% $\text{Na}_2\text{SiO}_3 \cdot 5\text{H}_2\text{O}$ proportion in the mix varies between 0.8 and 1.0
2	SSP:CC =0.7 (mass ratio of $\text{Na}_2\text{SiO}_3 \cdot 5\text{H}_2\text{O}$ solution to calcined clay)	$\text{Na}_2\text{SiO}_3 \cdot 5\text{H}_2\text{O}$ solution consisting of 54.5% solid	Alkali activator type
	SS:CC=0.7 (mass ratio of Na_2SiO_3 solution to calcined clay)	Na_2SiO_3 solution consisting of 54.5% solid	
	SH:CC = 0.7 (mass ratio of NaOH solution to calcined clay)	NaOH solution made up of 32% solid	

3	CC - 54.5SS	High viscosity Na ₂ SiO ₃ consisting of 54.5% solid	Ratio of mass of calcined clay to Na ₂ SiO ₃ solution
---	-------------	---	---

CC—calcined clay; SH—sodium hydroxide; SSP—sodium silicate pentahydrate; SS—sodium silicate

Preparation of the various mortar mixes was carried out using a 5 Litre Hobart mixer. The binder was prepared and shear mixed for about 5 minutes to ensure that the solution has penetrated all the layered sheets of the calcined clay for effective reaction. The quartz sand was then added until a homogenous mix was achieved. The mixes were then placed in the 50 mm x 50 mm steel cubes moulds and compacted uniformly using the vibration table, as specified by [32]. The samples were then demoulded after 24 hrs and cured in the air or sealed condition as required for the various mixes. The sealed cured specimens were wrapped in a cling film, stored in air-tight plastic box with some water at the bottom, in the conditioning room until testing. The temperature and relative humidity were maintained at 20°C and >95% respectively.

Table 3: Mortar mixes (kg per m³)

Group 1	Sand	CC – 32SH			CC – 44.1SSP		
L:B		Calcined clay	32% NaOH solution	Free water	Calcined clay	44.1% Na ₂ SiO ₃ .5H ₂ O	Free water
0.8	723	723	579	0	723	579	0
0.85	711	711	604	0	711	604	0
0.9	698	698	628	0	698	628	0
0.95	686	686	652	0	686	652	0
1	675	675	675	0	675	675	0
Group 2	Sand	Calcined clay	32% NaOH solution	54.5% Na ₂ SiO ₃ /5H ₂ O	Free water		
SSP:CC =0.7	1482	484	0	344	64		
SS:CC =0.7	1482	484	0	344	64		
SH:CC = 0.7	1482	484	344	0	64		

Group 3	Sand	Calcined clay	54.5% Na₂SiO₃	Free water
0.5	1221	396	198	84
0.75	1221	339	255	84
1	1221	297	297	84
1.25	1221	264	330	84
1.5	1221	238	356	84

2.3 Tests

The compressive strength for the three replicates (surface-saturated 50 mm x 50 mm mortar cubes samples for each mix) was determined at 7 and 28 days based on the procedure specified by ASTM C109 /109M-20A [32]. A JJ Lloyd compression testing machine was used with a loading rate of 1 KN/s (0.4 MPa/s) that accommodates the lower strength of many of the samples.

Microstructures of the three mortar mixes that have mass ratios of 1:1 were examined. The fragments from the compressive strength tests on the 28 days cured samples were vacuum dried and the fractured surface were examined by Scanning Electron Microscopy (SEM) using a Jeol SEM instrument (JSM-6060LV model). The fragments were used in order to expose the fresh surface for the SEM examination [33]. In order to identify the various mineralogical phases in the mixes, XRD was carried out. The samples were collected on a Panalytical Empyrean system with a Co (1.7903Å) K α X-ray source. This Co X-ray has a longer wavelength than the commonly used Cu K α tubes (~ 1.54 Å), but it prevents the fluorescence that can occur from the Fe in the sample. Due to the presence of many weak and overlapping peaks in the samples, the experiment was run for 2hrs instead of shorter measurement, to obtain a more quality data at a 2-theta angle of 5 to 90°.

Furthermore, Fourier Transform Infrared (FTIR) spectroscopy was performed on the crushed fragments of the mortar samples using Nicolet 6700 FT-IR. This test confirms the molecular fingerprints of a geopolymer matrix by measuring the amount of light absorbed by the bonds of vibrating molecules [34]. Background data was first obtained using the OMNIC software before

placing the specimen under the testing chamber of the equipment. The data for all the samples examined was obtained for a range of 600-4000 cm^{-1} wavelength. The output of the FTIR reported is wavelength in cm^{-1} against transmittance in percentage.

The density of three replicate geopolymer mortar cubes were determined at 7 and 28 days for the selected mix that yielded the highest strength, using a specific gravity balance based on the Archimedes principle and the mean density was then computed and reported. Further characterization of the calcined clay geopolymer mortar mix that yielded the highest strength was carried out through testing of the setting time, rheology and Ultrasonic Pulse Velocity (UPV).

The initial and final setting times of the mortar were determined based on the procedure specified by ASTM C191 – 19 [35]. The calcined clay geopolymer pastes that correspond to that of the peak strength mix with and without added free water were used. At regular time intervals, the penetration of the standard 1 mm needle on the sample was measured, until a penetration of 25 mm was achieved. The elapsed time between the initial mixing of the paste and the penetration of 25 mm was computed as the initial setting time of the mix. The final time of setting of the paste was calculated as the elapsed time between the initial mixing of the paste and the first measured penetration that did not mark the specimen surface with the needle.

The consistency of the peak strength mortar mix was determined using flow table test as described in BS 6463-103:1999 [36]. According to [37], workability of geopolymers are best characterized through determination of their rheological parameters against the widely used single point tests. Consequently, yield stress and plastic viscosity were measured using a Rheology International Series 2 viscometer Model RI:2:M. The rheometer was operated by rotating its spindle in the fresh mortar which measured the torque that overcomes the viscous resistance to the movement. The four-blade vane spindle had four rectangular blades of radius, $R_v = 9.5$ mm, and height $h = 38$ mm and was placed in a container of radius, 27.5 mm mounted in the middle of the lower plate.

3. Results and Discussion

3.1. Effect of liquid-to-binder mass ratios on the compressive strength

The compressive strength of the tested group 1 mixes are presented in figure 1. Due to the platy shape and layered structure of the calcined clay, a high L/B of between 0.8 and 1 was

used in order to produce a homogenous workable mortar for this group of mixes. The result shows strength development of the mortar for all the group 1 mixes with increase in testing age, which indicated continuity of the reaction (dissolution of residual raw materials and gel formation) in the air cured samples. The strength peaked at L/B ratio of 0.80 and dropped significantly as the ratio was increased to 1. The L/B ratio of 0.80 was thought to have sufficient activator content to enable dissolution of aluminate and silicate from the precursor, while not hindering the coagulation and polycondensation rate during the gel synthesis. On the other hand, increasing the L/B ratio resulted in decrease in strength of the mortar due to presence of excess activator that may not all be consumed in the reaction which caused voids in the microstructure as the sample solidifies in the air. Also, the high Na_2O content in the system resulting from increasing the activating solution proportion caused the excess Na^+ content to react with CO_2 by atmospheric carbonation. Thus, the geopolymerization process is disrupted and may have led to reduction in the strength. Although increasing the amount of alkali solution ensured a higher dissolution rate of the residual raw materials, but hindered the polycondensation rate by making the diffusion of dissolved species difficult.

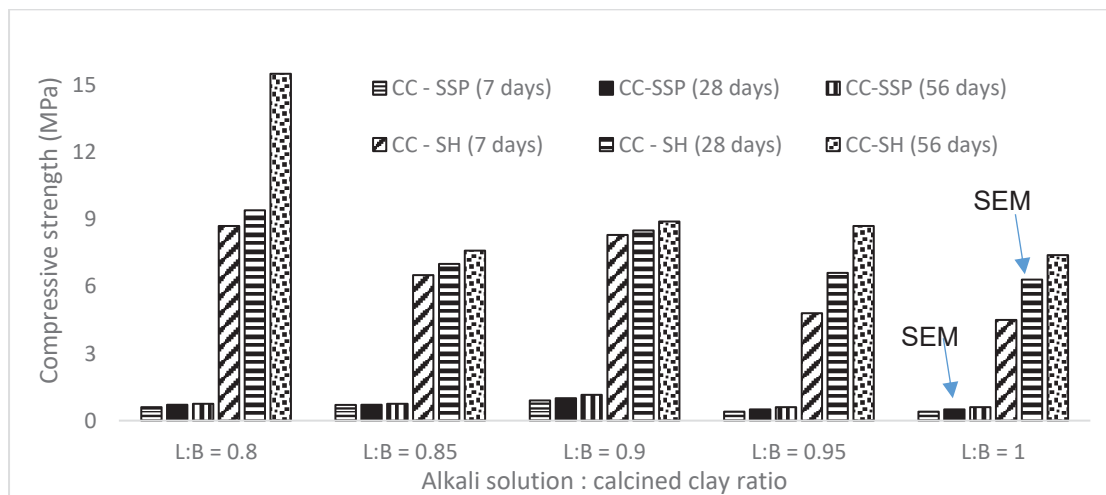


Figure 1: Compressive strength development of calcined clay geopolymer mortars activated by variable proportion of 2 types of chemical activators

The results presented in figure 1 further shows that significantly higher strength mortar is achieved by the alkalination of the calcined clay with 8M NaOH solution compared to the hydrous sodium silicate solution (SSP) regardless of the age and proportion of the solution used in the mixes. The 32% NaOH solution has enhanced leaching ability that dissolved the silicate and aluminate in the calcined clay which enriched the binding phase [38]. Conversely,

the 44.1% $\text{Na}_2\text{SiO}_3 \cdot 5\text{H}_2\text{O}$ solution had reduced binding ability, due to the dilution caused by the chemically bound water. Additionally, the dissolution of solid $\text{Na}_2\text{SiO}_3 \cdot 5\text{H}_2\text{O}$ under normal atmospheric pressure condition is not very effective, thereby limiting the availability of free silicate in the system that is required for the geopolymerization process. However, a recent study by [39] showed that a calcined smectite clay activated with blended $\text{Na}_2\text{SiO}_3 \cdot 5\text{H}_2\text{O}$ and $\text{Na}_3\text{C}_6\text{H}_5\text{O}_7$ produced a normal strength mortar in the presence of waste CaCO_3 .

3.2 Effect of alkali activator type on the compressive strength

Figure 2 present the results of the compressive strength for the group 2 mixes designed with equal alkali solution to calcined clay mass ratio of 0.7, but using 8M NaOH solution, commercially available, high viscosity water glass and sodium metasilicate pentahydrate dissolved solution. The results show that the compressive strength of the mortar activated by the high viscosity sodium silicate solution at both 7 and 28 days, is more than double that of the 54.5% $\text{Na}_2\text{SiO}_3 \cdot 5\text{H}_2\text{O}$ dissolved solution. The significant strength difference was caused by the variation in the amount of Na_2SiO_3 solid in the two chemical activators. This variation resulted in varying considerably the alkali modulus (ratio of $\%\text{SiO}_2$ to Na_2O), alkali dosage (ratio of $\%\text{Na}_2\text{O}$ to calcined clay), *etc* in the system, despite the two mixes having the same mass ratio of activator solution to calcined clay. Also, the chemically bound water in the SSP activator contributed in the dilution of the solution, thereby decreasing its binding effect. This is in agreement with the findings of [40] that low strength binder is achieved by activating precursors with hydrated chemical activator. On the other hand, the sodium hydroxide activated mortar achieved the highest strength for the group 2 mixes based on the mass ratio of 0.7 due to the higher Na:Al ratio induced in the system by the activator. However, for this group of mixes which are cured in sealed conditions, the strength achieved is low and is thought to be caused by the insufficient amount of chemical activator in the mix that will provide the required alkali dosage and modulus. The results in figures 1 and 2 stressed the fact that hydrous metasilicate and sodium hydroxide solutions produced non-geopolymer mortar based on this precursor. Liquid to binder ratio therefore has to be formulated to satisfy the prescribed molar oxide ratios for geopolymer mortar to be achieved as presented in the next section.

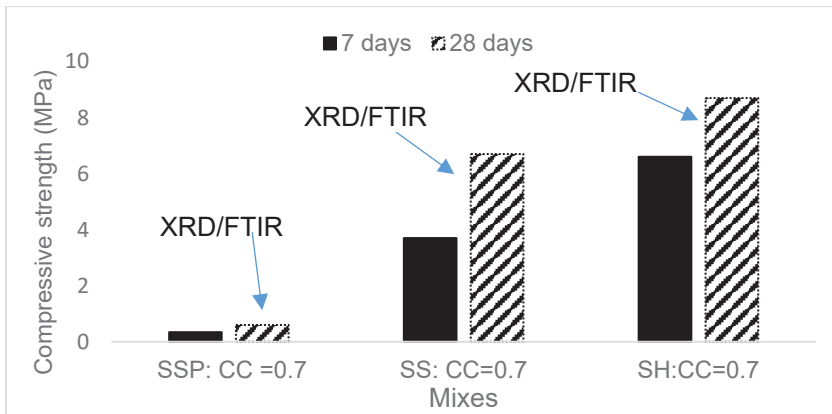


Figure 2: Compressive strength development of calcined clay geopolymer mortars activated by the three types of activators

3.3 Effect of sodium silicate solution to calcined clay mass ratio on the compressive strength

Due to the relatively low strength achieved by group 1 and 2 mixes that were formulated based on activating solution demand, the effect of the variable proportion of silicate solution (group 3) that have Si:Al and H₂O:Na₂O ratios within the optimal literature range were studied to determine which mass ratio (mix) will yield the peak strength. The tested samples, which were sealed cured showed increase in strength with age for all mass ratios, with a rapid strength, increase between 2 and 7 days as shown in figure 3.

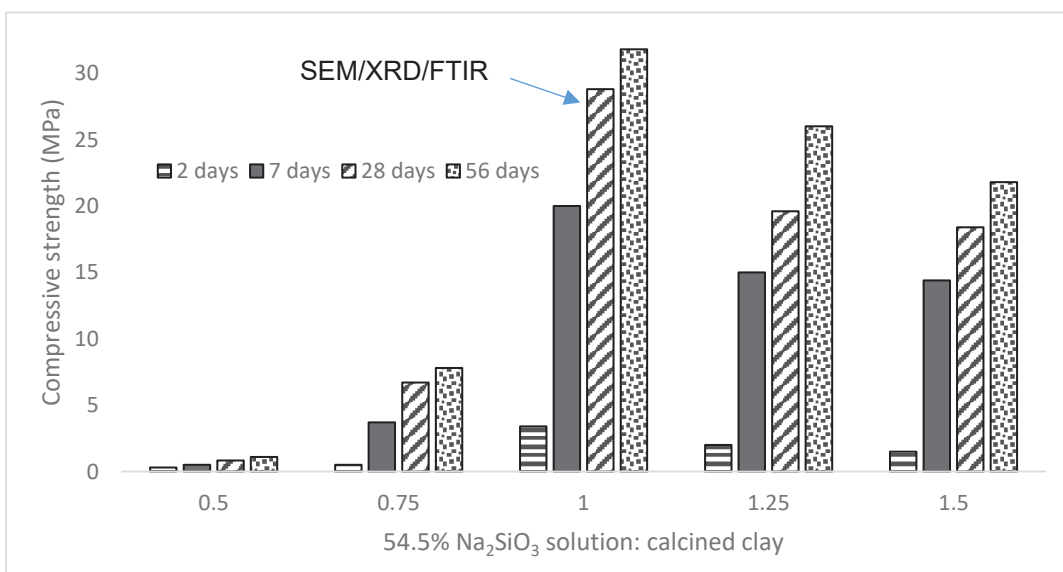


Figure 3: Compressive strength development of calcined clay geopolymer mortar activated by varied proportion of 54.5% sodium silicate solution

It can be seen that at 7 days, the geopolymer mortars had already achieved most of their strength due to advancement of the geopolymerization reaction in the system. Also, peak strength at all ages was achieved by the mass ratio of 1, which may have had sufficient alkali modulus and dosage that was required for the reaction. Increasing the mass ratio above 1 may have precipitated more than the required free silicate which disrupt the reaction and resulted in the decrease strength. This finding concur with [41,42] who concluded that a deterioration in strength is expected with increasing Na_2SiO_3 solution beyond the optimum. This was due to the hindering of the geopolymerization reaction through the Al–Si phase precipitation that prevented contact between the reacting materials and the activating solution. On the other hand, the low mass ratio below 1 may have yielded insufficient free silicate that was required to complete the geopolymerization, which resulted in a low strength mortar.

Moreover, from the molar oxide ratios calculated for this group of mixes presented in table 4, it can be seen that the mix that achieved the peak strength has $\text{SiO}_2/\text{Al}_2\text{O}_3$ and $\text{Na}_2\text{O}/\text{Al}_2\text{O}_3$ molar ratios of 4.12 and 1.0 respectively, which correspond to the ideal ratios prescribed by [14]. Also, the $\text{Na}_2\text{O}/\text{SiO}_2$ of 0.24 and $\text{H}_2\text{O}/\text{Na}_2\text{O}$ of 14.10 for the highest strength mix are similar to the optimum strength composition values reported by [18]. In summary, the strength achieved by the mixes presented in figure 3 reached a maximum and then decreased gradually due to the sensitivity of the geopolymer synthesis to variation in the molar oxide composition. Consequently, even though the molar oxide ratios of all the mixes fall within the range specified by [14], a significant difference in strength was observed, which stressed the need for mix optimization in geopolymers.

Table 4: Molar oxide ratios for the group 3 mixes

Mix - CC : SS ratio	$\text{Na}_2\text{O}/\text{Al}_2\text{O}_3$	$\text{SiO}_2/\text{Al}_2\text{O}_3$	$\text{Na}_2\text{O}/\text{SiO}_2$	$\text{H}_2\text{O}/\text{Na}_2\text{O}$
0.5	0.5	3.07	0.16	16.69
0.75	0.7	3.51	0.2	12.22
1	1	4.12	0.24	14.10
1.25	1.25	4.64	0.27	13.58
1.5	1.49	5.16	0.29	13.24

Comparing the results presented in figures 3 and 2, a very significant difference in strength can be clearly seen between the 54.5% Na_2SiO_3 solution and the hydrous $\text{Na}_2\text{SiO}_3 \cdot 5\text{H}_2\text{O}$ solution activated calcined clay mortars. In fact, no meaningful strength was achieved by activating the calcined clay with both 44.1% and 54.5% $\text{Na}_2\text{SiO}_3 \cdot 5\text{H}_2\text{O}$ solutions. Also, from further comparison of the results presented in figures 1 and 3, it was observed that seal curing enhanced the strength of geopolymer mortar compared to air curing by limiting carbonation that caused decline in strength. It also prevented cracks propagation and pores associated with rapid loss of moisture in the samples [43].

3.4 Microstructure

3.4.1 The morphology

The SEM image for the CC – 32SH mortar prepared with 8 M NaOH solution to calcined clay mass ratio of 1:1 cured under sealed conditions for 28 days is presented in figure 4. The micrograph reveals a densified and packed structure (a), as well as pores (c), which may be associated with the low strength achieved by the mix. The result further shows precipitation of a sponge-like, globular morphology on the surface resulting from the alkali activation.

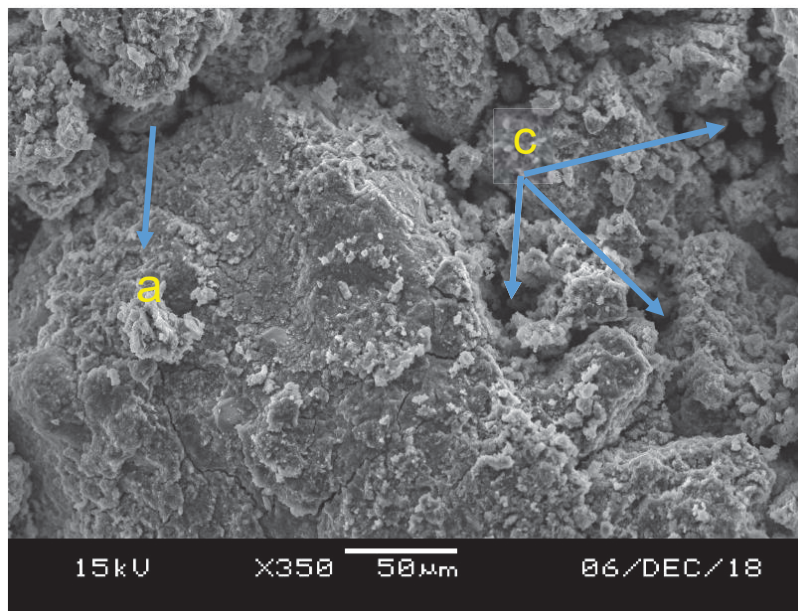


Figure 4: SEM micrograph for CC – 32SH mortar

Figure 5 presents the SEM image obtained for the 28 days sealed cured CC – 44.1SSP mortar which shows the presence of residual particles (a) in the bulk, undensified and uncompacted,

discrete structure which is thought to be the cause of the very low strength measured for this mix. The heavy presence of the residual unreacted calcined clay particles might have prevented the development of a uniform geopolymer network throughout the sample. The loose and dispersed structure was probably caused by the partial dissolution of the granular sodium silicate pentahydrate that was dissolved under normal atmospheric conditions. This is in addition to the dilution effect of the chemically bound water in the activator that may have hindered the dissolution of the residual raw materials and the precipitation of free silicate that will form the Si-O-Al polymeric network.

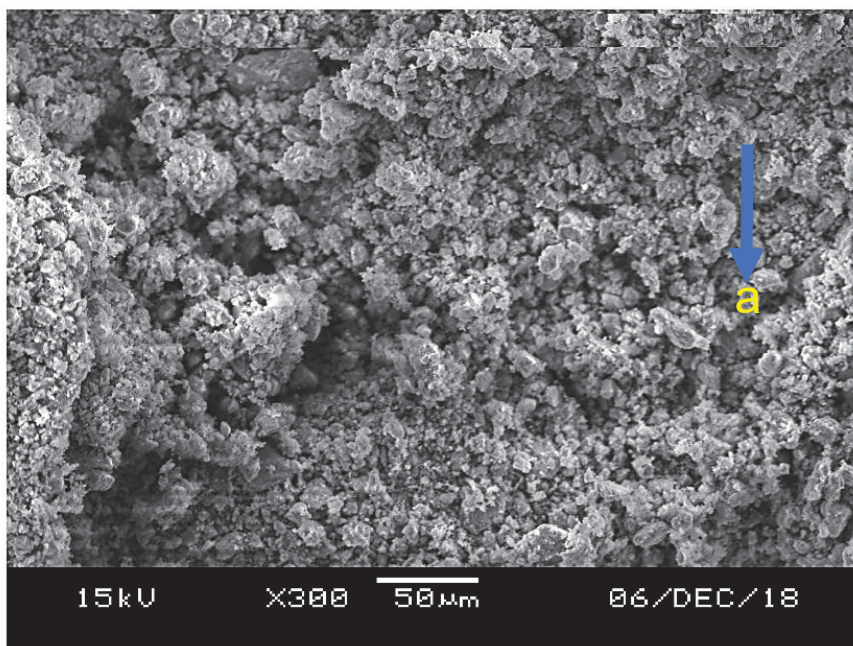


Figure 5: SEM micrograph for CC – 44.1SSP mortar

The microstructure of the CC - 54.5SS mortar prepared with the 54.5% Na_2SiO_3 solution to calcined clay mass ratio of 1:1 cured for 28 days under sealed conditions is shown in figure 6. It reveals a compact mass, bulk geopolymer structure (a glassy-like appearance with some sharp edges) which resulted in the high strength mortar. Sponge-like with globular units geopolymer gel which are precipitated during the reaction appear on the surface of the matrix (a). This is in agreement with the findings of [44] that the microstructure of low purity metakaolin geopolymers cured at ambient condition was consolidated enough to give high compressive strength.

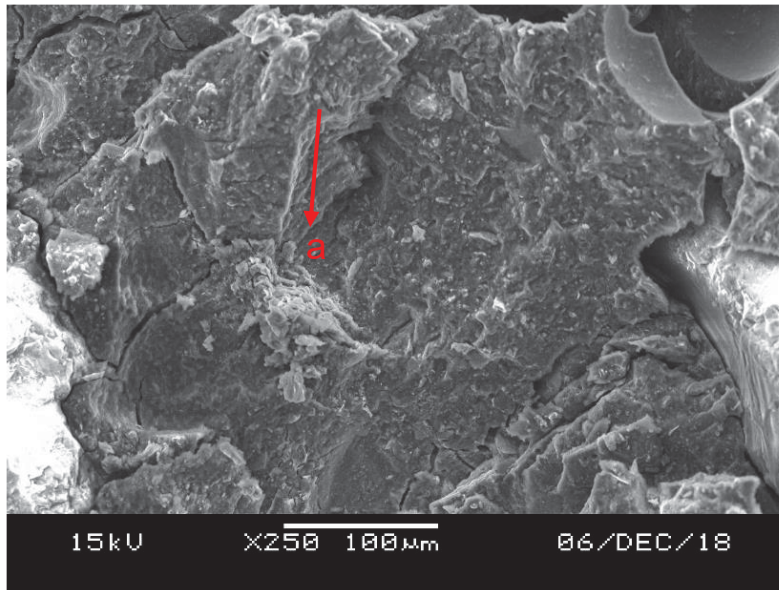


Figure 6: SEM image for CC - 54.5SS mortar

Comparing the SEM micrographs presented in figures 4-6, it was evident that the resulting mortar of Mix CC – 44.1SSP consisted of more unreacted calcined clay and voids than Mix CC - 54.5SS. It is also clear that the use of 54.5% sodium silicate solution is attributed with the increase in soluble silicate in the geopolymer system. This caused the development of compact and dense structure due to the soluble silicate that enhanced the depolymerisation of the aluminosilicate and subsequent precipitations of more geopolymer gels.

3.4.2 The mineralogical phases

Figure 7 shows that the calcined clay powder and its sodium silicate activated geopolymer paste exhibited similar peaks and amorphous humps at the various 2θ positions. However, at all the 2θ angles, the paste had a lower intensity compared to the raw calcined clay: except at the location $32\text{--}36^\circ 2\theta$ for the $\text{Co}(K\alpha)$. The amorphous halo at this location in the paste can be assigned to the geopolymer matrix. This phase is similar and conforms to the geopolymer matrix at the location $27 - 29^\circ 2\theta$ for $\text{Cu}(K\alpha)$ that was defined by [45]. The slight shift to the right of the location was caused by the $\text{Co}(1.7903\text{\AA}) K\alpha$ x-ray source used in this study as they had a longer wavelength than the $\text{Cu} K\alpha$ tubes ($\sim 1.54 \text{\AA}$) used by the referenced authors. The effect of this change of wavelength is, by Bragg's law, to shift the peaks to higher angles and can be seen in this context. Furthermore, the similarity of the XRD spectra in figure 7 is an indication that the various crystalline materials in the calcined clay did not seem to have fully reacted in the geopolymerisation. This is in agreement with previous study [46][8].

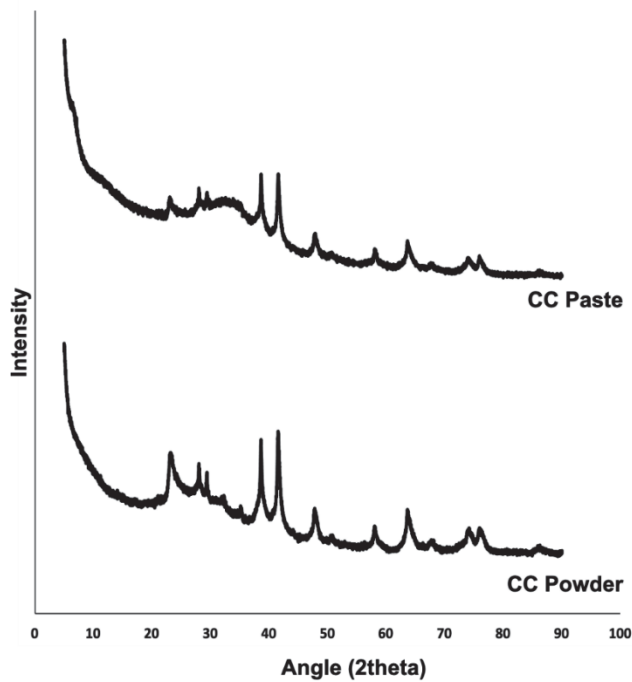


Figure 7: Comparing the XRD spectra of raw calcined clay and its geopolymeric paste

The XRD spectra of the group two samples - SSP 0.7, SH 0.7 and SS 0.7 are presented in figure 8. The geopolymeric activity of the samples were evaluated based on the peak intensity of some of the phases in the samples. It can be observed from the figure 8 that, the Quartz peaks of the sample at 2-theta angle of 24.2° and 31° is highest in the SSP 0.7 mix due to the weak binding of the sand in the system. Analysis of the sodium hydroxide activated calcined clay mortar showed the zeolites peaks at 2-theta angle of 8.3, 27.9 and 35.9°, as well as muscovites (from the unreacted precursor) intensity peaks at 2-theta angle of 31 and 36°. These minerals phases are a result of the effective dissolution of the precursor by the 32% NaOH solution, which produced the less stable N-A-S-H in the system. The spectra for the SS 0.7 shows the geopolymer matrix – Na/K – Al – Si – O intensity peak at 32.5, 46 and 58°, as well as hematites peaks at 2-theta angle of 49°.

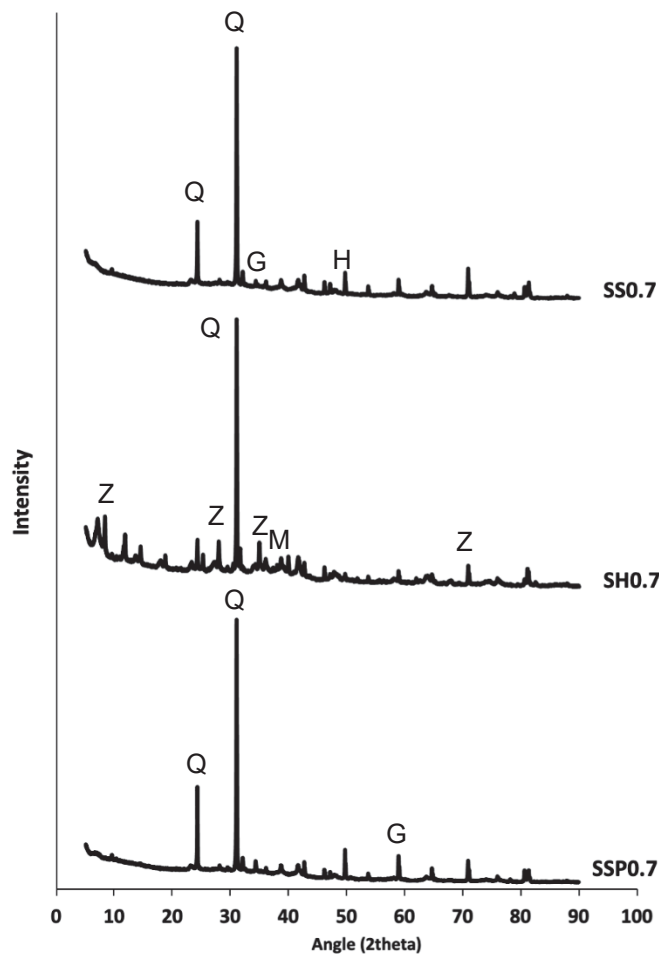


Figure 8: XRD spectra of group two mortar mixes at 28 days

(Z is zeolite, M is muscovite, G is Geopolymer matrix, Q is Quartz, H is hematite)

The summary of the phases in the group 2 mixes which were obtained by analysing the result with the expert data base system of the XRD machine are presented in table 5.

Table 5: Summary of the mineralogical phases in three of the mixes

Mineral	Chemical formula	CC	SSP	CC	SH	CC	SS
		0.7	0.7	0.7			
Hematite	Fe_2O_3	X		x		X	
Quartz	SiO_2	X		x		X	
Muscovite	$\text{K}_{0.92}\text{Na}_{0.08}\text{Al}_{1.88}\text{Fe}_{0.12}\text{Mg}_{0.04}(\text{Al}_{1.08}\text{Si}_{2.92}\text{O}_{10})(\text{OH})_{1.89}\text{F}_{0.11}$	X		x		X	
Zeolite	$\text{Na}_{24}\text{Al}_{24}\text{Si}_{24}\text{O}_{96}(\text{H}_2\text{O})_{64.8}$			x			
Na/K-Si-O-Al-O	Na/K (AlSi_3O_8)						X
Calcite	CaCO_3						X

Blodite	$\text{Na}_2\text{Mg}_4(\text{SO}_4)_4(\text{H}_2\text{O})$	x
Kaolinite	$\text{Al}_2\text{Si}_2\text{O}_5(\text{OH})$	X

The albite and sanidine mineral frameworks identified in figure 9 are geopolymeric frameworks that are similar to the Na-Poly(sialate-disiloxo) and K-Poly(sialate-disiloxo), as reported by [14]. These geopolymeric frameworks have a Si:Al of 3. Thus, figure 9 confirms that the calcined lateritic clay geopolymer is only partially crystalline, containing ordered domains with structures similar to the Na-feldspar, albite and the K-feldspar, sanidine.

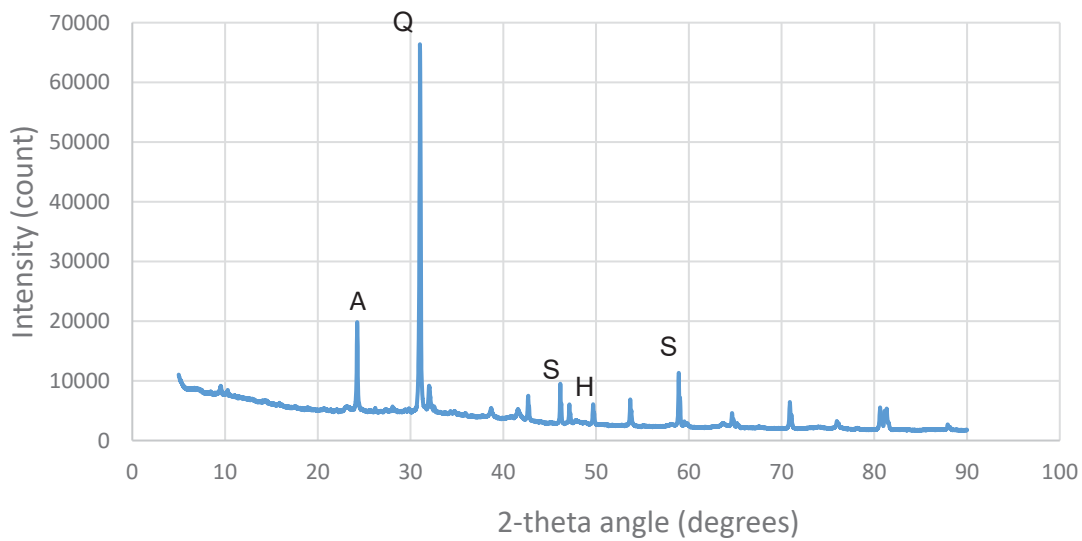


Figure 9: XRD for the CC SS 1 mortar at 28 days

(A is anatase; S is Sanidine; Q is Quartz; H is hematite)

3.4.3 The functional groups

Figure 10 presents the IR curves for the group two mortar samples - mixes SSP 0.7, SH 0.7 and SS 0.7, as well as that of the peak strength mortar – mix SS 1.0. The Si-O vibration band generated by the SiO_4 groups in the SS 1 mortar can be seen at around 950 cm^{-1} , due to the formation of a sodium aluminosilicate type gel. The band at around 1350 cm^{-1} was attributed to the stretching vibrations generated by the Al-O bonds in the AlO_4 groups. The bending vibrations generated by the OH groups in the water caused the band at 3250 cm^{-1} . These bending and stretching peaks are indicative of the geopolymeric structure. This can be inferred from the findings of [47], who suggested that the bonding exhibited at the band around 966 cm^{-1} indicates the Si-O stretching vibration of SiO_4 and AlO_4 of geopolymer and N-A-S-H gel.

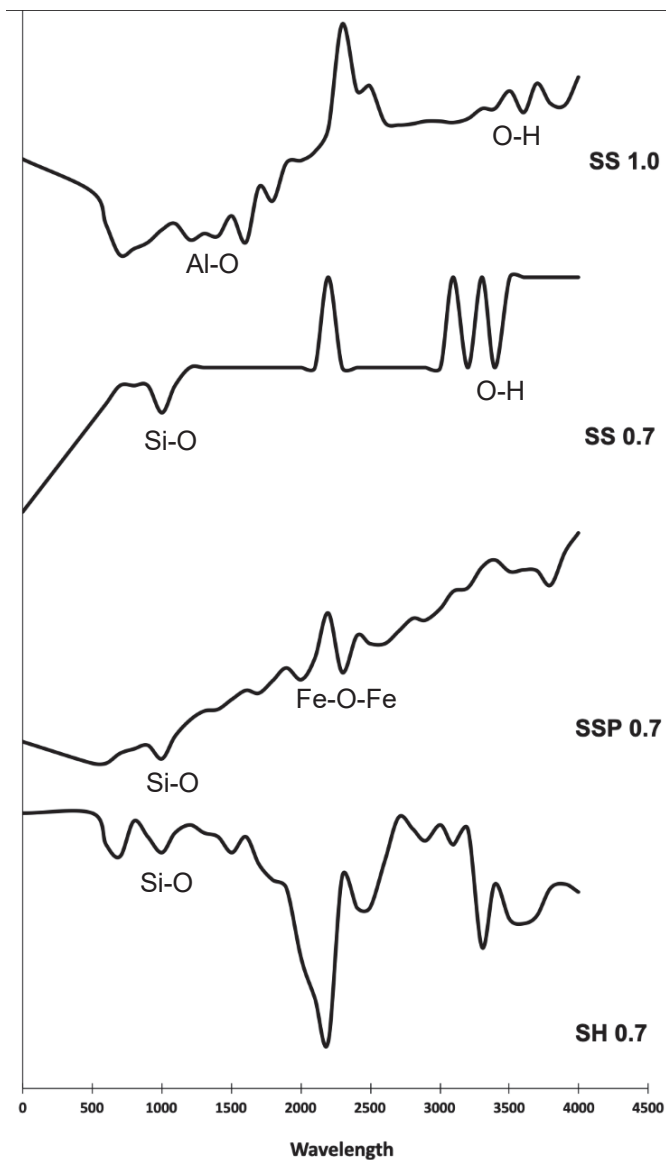


Figure 10: IR curves for the group two (SSP 0.7, SS 0.7, SH 0.7) and peak strength (SS 1.0) mortars

For the SSP 0.7 system shown in figure 10, the decrease in the peak in the region of 950 cm^{-1} which is assigned to the Si – O stretching, can be attributed to the partial and weak nature of the geopolymerisation reaction. The Fe – O – Fe stretching was found at 2350 cm^{-1} in the IR curve. This indicates that the hematite remained in the hardened sample even after activating the calcined clay with the sodium silicate pentahydrate solution.

For the SH 0.7 synthesized mortar, the broad band in the region of 1645 cm^{-1} and the peak at $3,250\text{ cm}^{-1}$ can be assigned to the O-H bonding of water in the system, as shown in figure 10. The narrowing of the Si-O symmetrical stretch is caused by the strong dissolution of the

aluminosilicate in the calcined clay. This may be the reason for the weak binding phase characterized by the high Na:Si composition of the mix.

3.5 The density and Ultrasonic Pulse Velocity (UPV) of the peak strength mortar mix

The density measured for the peak strength mortar – mix SS 1.0 decreased with increase in curing age due to the hardening and drying of the samples that was characterized by the loss of moisture. At 7 and 28 days, the density computed was 2191 kg/m³ and 2122 kg/m³ respectively, which can be described as normal weight mortar.

The computed UPV for the peak strength calcined clay geopolymer mortar – SS 1.0 at 7 and 28 days were 2.3 km/s and 2.4 km/s, respectively. This increase in the measured pulse velocities (i.e a shorter signal travel time through the sample) with an increase in curing age of the peak strength mortar is an indication of enhance dense internal structure of the sample due to advancement of the geopolymerization reaction. The UPV results also showed that at both 7 and 28 days, the values obtained correlate with the compressive strength development of the mortar sample. These trends concur with the findings of [48].

3.6 The setting time and rheology of the geopolymer paste

The setting time indicated the early strength development of the geopolymer paste of the two mixes that had Liquid to Binder ratios (sum of alkali solution and free water divide by the calcined clay) of 1.3 and 1. These paste mixes correspond to the peak strength mortar – SS 1.0 (calcined clay to sodium silicate solution mass ratio of 1) with and without added water respectively. The measured setting times were very long for the calcined clay based geopolymer pastes compared to what is obtainable from traditional Portland cement paste. The initial setting time was 7.5 hrs, while the final setting time was 8.25 hrs for the mix that has L:B of 1. Also, by increasing the L:B of the geopolymer paste to 1.3 through addition of free water, the initial and final setting times increased to 10.25 hrs and 11 hrs respectively. This concur with [49] who reported that, the setting process of geopolymers derived from calcined lithomarge takes several hours. However, a relatively short setting time was achieved by [25] by blending calcined clay with GGBS that supplied calcium into the system and thereby lowered the setting times through quick precipitation of C(N)-A-S-H gel. It can be seen that the two geopolymer pastes produced, hardened and gained sufficient strength such that they could be

demoulded within 20 hrs when cured at room temperature. This hardening behaviour is desired for the daily turnaround of moulds especially in precast industries. Also, the delayed setting times may be useful in the transportation and handling of the calcined clay based geopolymer concrete, especially in applications where extended workability is required.

The measured spread for the peak strength mortar – SS 1.0 mix is 175 mm. This flow indicate the workable character of the mortar which is influenced by the H₂O:Na₂O of 14.1 of the mix.

Moreover, a consistent and controlled rheology that can be describe by the Herschel-Bulkley (power law) model was achieved by the calcined clay geopolymer grout which has L:B of 1.3. The shear stress τ , was computed from the measured torque based on equation 1 specified by [50].

$$\tau = 3T/(2\pi (Rv^3 + 3Rv^3h)) \quad (1)$$
 where, T is the torque; τ is the shear stress; Rv = 9.5 mm is the radius of the four rectangular blades, and h = 38 mm is their height;

At a shear rate of 40 S⁻¹, the grout shear stress measured was 4.20 Pa and the viscosity was 241 PaS. At the shear rate of 20 S⁻¹, the grout shear stress was 4.01 Pa and the viscosity was 133.4 PaS. The measured shear stress of the grout was influenced by both the high H₂O/Na₂O ratio of 14.1 and L:B of 1.3. [51] obtained almost similar rheological properties for a flash calcined clay activated by potassium silicate solution. The high plastic viscosity measured was due to the viscous nature of the sodium silicate solution used as the alkali metal source for the grout.

4. Conclusion

From the results reported in this paper, it can be concluded that:

1. Low strength mortar was achieved by activating the calcined clay with sodium silicate solution derived from the dissolution of granular sodium silicate pentahydrate under normal atmospheric conditions. This decreased strength resulted from the reduced alkalination potential of the silicate solution due to the dilution caused by the chemically bound water. Also, limited free silicate ions were incorporated in the solid during the geopolymerization process, caused by the partial dissolution of the hydrous sodium silicate. As such, low strength non-geopolymer matrix was precipitated which has unreactive residual calcined clay that prevented complete development of the geopolymer network;

2. Geopolymer synthesis of the calcined clay shows high sensitivity to the variation in molar oxide ratios. Whereas, all the mixes prepared with the 54.5% sodium silicate solution have molar ratios that fall within the range specified by different authors, the strength obtained reached a maximum and then decreased subsequently with the variation in the molar oxide composition. In this study, the mix that achieved the peak strength at all ages has $\text{SiO}_2/\text{Al}_2\text{O}_3$, $\text{Na}_2\text{O}/\text{Al}_2\text{O}_3$, $\text{Na}_2\text{O}/\text{SiO}_2$ and $\text{H}_2\text{O}/\text{Na}_2\text{O}$ molar ratios of 4.12, 1, 0.24 and 14.1 respectively;
3. Sealed curing conditions enhance the strength of the calcined clay geopolymer mortars by limiting the effects of carbonation, regardless of the proportion or type of chemical activator used;
4. The microstructure of the calcined clay geopolymer mortar is dense and compact with sponge-like, globular morphology on the surface of the matrix.
5. The calcined clay geopolymer mortar is only partially crystalline, containing ordered domains with structures similar to the Na-feldspar, albite and the K-feldspar, sanidine. These are the geopolymeric frameworks that are similar to Na-Poly(sialate-disiloxo) and K-Poly(sialate-disiloxo) respectively. These geopolymeric frameworks have Si:Al of 3. The XRD result further revealed zeolites phases for the 32% NaOH activated mix, which was caused by the rapid dissolution of the silicate and aluminate component of the calcined clay in the system.
6. Distinct broad peaks assigned to the Si–O, Al–O, O–H and Fe–O–Fe have been identified in the peak strength calcined clay geopolymer mortar. The broad Al–O and Si–O peaks are the major fingerprints of an aluminosilicate geopolymeric matrix.

References

- [1] K.L. Scrivener, V.M. John, E.M. Gartner, Eco-efficient cements: Potential economically viable solutions for a low-CO₂ cement-based materials industry, *Cem. Concr. Res.* 114 (2018) 2–26. <https://doi.org/10.1016/j.cemconres.2018.03.015>.
- [2] J.L. Provis, Alkali-activated materials, *Cem. Concr. Res.* 114 (2018) 40–48. <https://doi.org/10.1016/j.cemconres.2017.02.009>.
- [3] A. Heath, K. Paine, M. McManus, Minimising the global warming potential of clay based geopolymers, *J. Clean. Prod.* 78 (2014). <https://doi.org/10.1016/j.jclepro.2014.04.046>.
- [4] A.C. Heath, K.A. Paine, M.C. Mcmanus, Minimising the global warming potential of clay based geopolymers, *J. Clean. Prod.* 78 (2014) 75–83. <https://doi.org/10.1016/j.jclepro.2014.04.046>.
- [5] A. Elimbi, H.K. Tchakoute, D. Njopwouo, Effects of calcination temperature of kaolinite clays on the properties of geopolymer cements, *Constr. Build. Mater.* 25 (2011) 2805–2812. <https://doi.org/10.1016/J.CONBUILDMAT.2010.12.055>.
- [6] D. Zhou, R. Wang, M. Tyrer, H. Wong, and C. Cheeseman, Sustainable infrastructure development through use of calcined excavated waste clay as a supplementary cementitious material, *J. Clean. Prod.* 168 (2017) 1180–1192. <https://doi.org/10.1016/j.jclepro.2017.09.098>.
- [7] R.F. Lopez, *Calcined Clayey Soils as a Potential Replacement for Cement in Developing Countries*, Lausanne, EPFL, 2009. <https://doi.org/http://dx.doi.org/10.5075/epfl-thesis-4302>.
- [8] C.R. Kaze, H.K. Tchakoute, T.T. Mbakop, J.R. Mache, E. Kamseu, U.C. Melo, C. Leonelli, H. Rahier, Synthesis and properties of inorganic polymers (geopolymers) derived from Cameroon-meta-halloysite, *Ceram. Int.* 44 (2018) 18499–18508. <https://doi.org/10.1016/j.ceramint.2018.07.070>.
- [9] J. Davidovits, Red Geopolymer cement could become the standard, *Geopolymer Institute*. (2012).
- [10] G. Stoops, V. Marcelino, *Interpretation of Micromorphological Features of Soils and Regoliths*, Elsevier, 2018. <https://doi.org/10.1016/C2014-0-01728-5>.

- [11] A. R. Brough, A. Atkinson, Sodium silicate-based, alkali-activated slag mortars: Part I. Strength, hydration and microstructure, *Cem. Concr. Res.* 32 (2002) 865–879.
[https://doi.org/https://doi.org/10.1016/S0008-8846\(02\)00717-2](https://doi.org/https://doi.org/10.1016/S0008-8846(02)00717-2).
- [12] P. Duxson, A. Fernández-Jiménez, J. L. Provis, G. C. Lukey, A. Palomo, A. and J. S. J. Van Deventer, Geopolymer technology: The current state of the art, *J. Mater. Sci.* 42 (2006) 2917–2933. <https://doi.org/10.1007/s10853-006-0637-z>.
- [13] J.L. Provis, A. Fernández-Jiménez, E. Kamseu, C. Leonelli, A. Palomo, Binder chemistry – Low-calcium alkali-activated materials, *RILEM State-of-the-Art Reports.* 13 (2014) 93–123. https://doi.org/10.1007/978-94-007-7672-2_4.
- [14] J. Davidovits, *Geopolymer Chemistry and Applications*, 3rd ed., Geopolymer Institute, 2015.
- [15] C. Shi, B. Qu, J.L. Provis, Recent progress in low-carbon binders, *Cem. Concr. Res.* 122 (2019) 227–250. <https://doi.org/10.1016/j.cemconres.2019.05.009>.
- [16] D. Papias, I.P. Giannopoulou, T. Perraki, Effect of synthesis parameters on the mechanical properties of fly ash-based geopolymers, *Colloids Surfaces A Physicochem. Eng. Asp.* 301 (2007) 246–254.
<https://doi.org/10.1016/j.colsurfa.2006.12.064>.
- [17] B. Singh, G. Ishwarya, M. Gupta, S.K. Bhattacharyya, Geopolymer concrete: A review of some recent developments, *Constr. Build. Mater.* 85 (2015) 78–90.
<https://doi.org/10.1016/j.conbuildmat.2015.03.036>.
- [18] Y.M. Liew, C.Y. Heah, A.B. Mohd Mustafa, H. Kamarudin, Structure and properties of clay-based geopolymer cements: A review, *Prog. Mater. Sci.* 83 (2016) 595–629.
<https://doi.org/10.1016/j.pmatsci.2016.08.002>.
- [19] R. Vinai, M. Soutsos, Production of sodium silicate powder from waste glass cullet for alkali activation of alternative binders, *Cem. Concr. Res.* 116 (2019) 45–56.
<https://doi.org/10.1016/j.cemconres.2018.11.008>.
- [20] J.S. Falcone, J.L. Bass, M. Angelella, E.R. Schenk, K.A. Brensinger, The determination of sodium silicate composition using ATR FT-IR, *Ind. Eng. Chem. Res.* 49 (2010) 6287–6290. <https://doi.org/10.1021/ie1002747>.
- [21] J. Davidovits, Application of Ca-based geopolymer with blast furnace slag, a review,

in: B. Jones, P. T.; Pontikes, Y.; Elsen, J.; Cizer, O.; Boehme, L.; Gerven, T.; Geysen, D.; Guo, M. and Blanpain (Ed.), *Second Int. Slag Valorization Symp.*, Leuven, Belgium, 2011: pp. 1–18.

- [22] J.L. Provis, K. Arbi, S.A. Bernal, D. Bondar, A. Buchwald, A. Castel, S. Chithiraputhiran, M. Cyr, A. Dehghan, K. Dombrowski-Daube, A. Dubey, V. Ducman, G.J.G. Gluth, S. Nanukuttan, K. Peterson, F. Puertas, A. van Riessen, M. Torres-Carrasco, G. Ye, Y. Zuo, RILEM TC 247-DTA round robin test: mix design and reproducibility of compressive strength of alkali-activated concretes, *Mater. Struct. Constr.* 52 (2019) 1–13. <https://doi.org/10.1617/s11527-019-1396-z>.
- [23] P.S. Deb, P. Nath, P.K. Sarker, The effects of ground granulated blast-furnace slag blending with fly ash and activator content on the workability and strength properties of geopolymer concrete cured at ambient temperature, *Mater. Des.* 62 (2014) 32–39. <https://doi.org/10.1016/j.matdes.2014.05.001>.
- [24] J. Davidovits, Geopolymer Cement a review, *Inst. Geopolymer.* (2013) 1–11.
- [25] J. Kwasny, M.N. Soutsos, J.A. McIntosh, D.J. Cleland, Comparison of the effect of mix proportion parameters on behaviour of geopolymer and Portland cement mortars, *Constr. Build. Mater.* 187 (2018) 635–651. <https://doi.org/10.1016/j.conbuildmat.2018.07.165>.
- [26] A. McIntosh, S.E.M. Lawther, J. Kwasny, M.N. Soutsos, D. Cleland, S. Nanukuttan, Selection and characterisation of geological materials for use as geopolymer precursors, in: *Adv. Appl. Ceram.*, Maney Publishing, 2015: pp. 378–385. <https://doi.org/10.1179/1743676115Y.0000000055>.
- [27] M. Panizza, M. Natali, E. Garbin, S. Tamburini, M. Secco, Assessment of geopolymers with Construction and Demolition Waste (CDW) aggregates as a building material, *Constr. Build. Mater.* 181 (2018) 119–133. <https://doi.org/10.1016/j.conbuildmat.2018.06.018>.
- [28] ASTM International, ASTM C618-19, Standard specification for coal fly ash and raw or calcined natural pozzolans for use in concrete, 2019.
- [29] S. Donatello, M. Tyrer, C.R. Cheeseman, Comparison of test methods to assess pozzolanic activity, *Cem. Concr. Compos.* 32 (2010) 121–127.

<https://doi.org/10.1016/j.cemconcomp.2009.10.008>.

- [30] A. S. Bature, M. Khorami, E. Ganjian, and M. Tyrer, Effect of the nature of chemical activator on the compressive strength of calcined clay geopolymer mortar, in: Fifth Int. Conf. Sustain. Constr. Mater. Technol., 2019.
- [31] F. Messina, C. Ferone, A. Molino, G. Roviello, F. Colangelo, B. Molino, R. Cioffi, Synergistic recycling of calcined clayey sediments and water potabilization sludge as geopolymer precursors: Upscaling from binders to precast paving cement-free bricks, *Constr. Build. Mater.* 133 (2017) 14–26.
<https://doi.org/10.1016/j.conbuildmat.2016.12.039>.
- [32] ASTM International, ASTM C109 / 109M-20A Standard Test Method for Compressive Strength of Hydraulic Cement Mortars (Using 2-in. or [50-mm] Cube Specimens) 1, 2020. https://doi.org/10.1520/C0109_C0109M-20A.
- [33] US Department of transport, Petrographic Methods of Examining Hardened Concrete: A Petrographic Manual, Washington DC, 2006.
<https://www.fhwa.dot.gov/publications/research/infrastructure/pavements/pccp/04150/04150.pdf>.
- [34] K. Komnitsas, D. Zaharaki, A. Vlachou, G. Bartzas, M. Galetakis, Effect of synthesis parameters on the quality of construction and demolition wastes (CDW) geopolymers, *Adv. Powder Technol.* 26 (2015) 368–376. <https://doi.org/10.1016/j.appt.2014.11.012>.
- [35] ASTM International, ASTM C191-19, Standard Test Methods for Time of Setting of Hydraulic Cement by Vicat Needle, 2019.
- [36] British Standard Institution, BS 6463-103:1999 Quicklime, hydrated lime and natural calcium carbonate. Methods for physical testing, 1999.
- [37] A.I. Laskar, R. Bhattacharjee, Rheology of fly-ash-based geopolymer concrete, *ACI Mater. J.* 108 (2011) 536–542. <https://doi.org/10.14359/51683263>.
- [38] A. S. Bature, M. Khorami, E. Ganjian, and M. Tyrer, Influence of alkali solution on compressive strength of calcined clay and GGBS alkali activated mortar, in: M. Tyrer, E. Ganjian, and A. West (Ed.), 38th Cement Concr. Sci. Conf., 2018: p. Paper No. 16.
- [39] L. Valentini, S. Contessi, M.C. Dalconi, F. Zorzi, E. Garbin, Alkali-activated calcined smectite clay blended with waste calcium carbonate as a low-carbon binder, *J. Clean.*

- Prod. 184 (2018) 41–49. <https://doi.org/10.1016/j.jclepro.2018.02.249>.
- [40] S.A. Bernal, J.L. Provis, A. Fernández-Jiménez, P. V. Krivenko, E. Kavalerova, M. Palacios, C. Shi, Binder chemistry - High-calcium alkali-activated materials, RILEM State-of-the-Art Reports. 13 (2014) 59–91. https://doi.org/10.1007/978-94-007-7672-2_3.
- [41] Y. M. Liew, H. Kamarudin, A. M. Mustafa Al-Bakri, M.BnHussain, M. Luqman, I Khairul Nizar, C. M. Ruzaidi, and C. Y. Heah, Optimization of solids-to-liquid and alkali activator ratios of calcined kaolin geopolymeric powder, *Constr. Build. Mater.* (2012). <https://www.sciencedirect.com/science/article/pii/S0950061812005454> (accessed November 20, 2019).
- [42] A. S. Bature, M. Khorami, E. Ganjian, and M. Tyrer, Effects of Sodium Silicate Proportion on Strength Development of Calcined Clay Geopolymer Mortar, in: R. Ball, B. Dams, V. Ferrandiz-Mas, X. Ke, K. Paine, M. Tyrer, & P. Walker (Ed.), *39th Cem. Concr. Sci. Conf. 2019.*, University of Bath, UK, 2019: pp. 148–152. <https://doi.org/ISBN 978-0-86197-201-2>.
- [43] M. Kumar, S.K. Saxena, N.B. Singh, Influence of some additives on the properties of fly ash based geopolymer cement mortars, *SN Appl. Sci.* 1 (2019) 481. <https://doi.org/10.1007/s42452-019-0506-4>.
- [44] A. Elimbi, H.K. Tchakoute, M. Kondoh, J. Dika Manga, Thermal behavior and characteristics of fired geopolymers produced from local Cameroonian metakaolin, *Ceram. Int.* 40 (2014) 4515–4520. <https://doi.org/10.1016/j.ceramint.2013.08.126>.
- [45] J. Davidovits, R. Davidovits, *Ferro-sialate Geopolymers (-Fe-O-Si-O-Al-O-)*, 2020. <https://doi.org/10.13140/RG.2.2.25792.89608/2>.
- [46] S.E.M. Lawther, A. Mcintosh, S. V Nanukuttan, J. Provis, Understanding the microstructure of alternative binder systems-banahCEM, a metakaolin based geopolymer, in: *Civ. Eng. Res. Ireland.*, 2016. <https://www.researchgate.net/publication/309032394> (accessed March 9, 2020).
- [47] F. Puertas, M. Torres-Carrasco, M. M. Alonso, Reuse of urban and industrial waste glass as a novel activator for alkali-activated slag cement pastes: a case study, in: *Handb. Alkali Act. Cem. Mortars Concr.*, Woodhead, 2015: pp. 75–109.

- [48] A. Hamood, J.M. Khatib, C. Williams, The effectiveness of using Raw Sewage Sludge (RSS) as a water replacement in cement mortar mixes containing Unprocessed Fly Ash (u-FA), *Constr. Build. Mater.* 147 (2017) 27–34.
<https://doi.org/10.1016/j.conbuildmat.2017.04.159>.
- [49] J.A. Blackstock, J. M.; Neill, J. and McIntosh, Geopolymeric Concrete and methods of forming it from a basaltic precursor, EP 2 451 758 B1, 2017, 2017.
- [50] D.R. Banfill, P. F. G. and Kitching, Use of a controlled stress rheometer to study the yield stress of oil well cement slurries, in: *Rheol. Fresh Cem.*, 1990: pp. 125–136.
- [51] D. Geddes, J. L. Provis, S. A. Bernal, S. A. and M. Hayes, Effect of calcination method and clay purity on the performance of metakaolin-based geopolymers, in: *Int. Conf. Alkali Act. Mater. Geopolymers Versatile Mater. Offer. High Perform. Low Emiss.*, 2018.